

Modification of PET surfaces with Gum Arabic towards its bacterial anti-adhesiveness using an experimental factorial design approach

Tugce Caykara, José Silva, Sara Fernandes, Adelaide Braga, Joana Rodrigues, Ligia R. Rodrigues, Carla Silva



PII: S2352-4928(21)00676-0

DOI: <https://doi.org/10.1016/j.mtcomm.2021.102684>

Reference: MTCOMM102684

To appear in: *Materials Today Communications*

Received date: 19 February 2021

Revised date: 5 July 2021

Accepted date: 26 July 2021

Please cite this article as: Tugce Caykara, José Silva, Sara Fernandes, Adelaide Braga, Joana Rodrigues, Ligia R. Rodrigues and Carla Silva, Modification of PET surfaces with Gum Arabic towards its bacterial anti-adhesiveness using an experimental factorial design approach, *Materials Today Communications*, (2021) doi:<https://doi.org/10.1016/j.mtcomm.2021.102684>

This is a PDF file of an article that has undergone enhancements after acceptance, such as the addition of a cover page and metadata, and formatting for readability, but it is not yet the definitive version of record. This version will undergo additional copyediting, typesetting and review before it is published in its final form, but we are providing this version to give early visibility of the article. Please note that, during the production process, errors may be discovered which could affect the content, and all legal disclaimers that apply to the journal pertain.

© 2021 Published by Elsevier.

Modification of PET surfaces with Gum Arabic towards its bacterial anti-adhesiveness using an experimental factorial design approach

Tugce Caykara^{a,b}, José Silva^a, Sara Fernandes^a, Adelaide Braga^b, Joana Rodrigues^b, Ligia R. Rodrigues^b, Carla Silva^c

^a CENTI-Center for Nanotechnology and Smart Materials, Rua Fernando Mesquita 2785, 4760-034, Vila Nova de Famalicão, Portugal

^b CEB-Centre of Biological Engineering, Universidade do Minho, Campus de Gualtar, 4710-057 Braga, Portugal

^c CITEVE-Technological Center for the Textile and Clothing Industries of Portugal, Rua Fernando Mesquita 2785, 4760-034, Vila Nova de Famalicão, Portugal

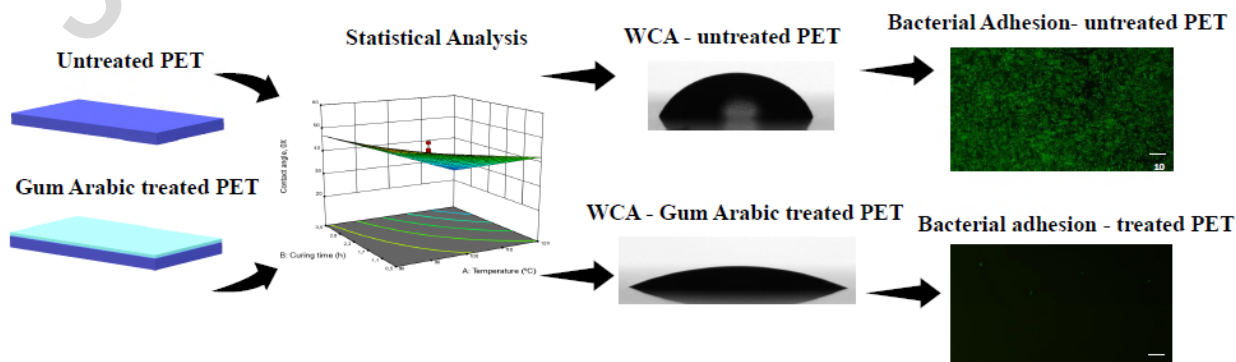
*Correspondence: Carla Silva, cjsilva@citeve.pt

Received: date; Accepted: date; Published: date

Abstract

Bacterial adhesion onto hospital material surfaces still represents a big healthcare issue, being preventive measures required to mitigate this problem, such as increasing material surface hydrophilicity. In the present study, gum Arabic, a hydrophilic polysaccharide, was used to modify the surface of polyethylene terephthalate (PET). Initial water contact angle (WCA) and WCA after several washing cycles were studied as response variables by a 2^4 full factorial design. Several reaction parameters, such as contact time between gum Arabic and PET, gum Arabic concentration, curing temperature and curing time for PET modification were investigated. The most significant parameters were found to be the curing temperature and curing time. The optimized parameters led to a WCA reduction from 70° to 27° . The modified PET samples were characterized using several techniques including AFM, colorimetric, ATR-FTIR and contact angle which further confirmed a successful surface modification. Furthermore, bacterial adhesion assays have clearly shown that the treated PET material was highly effective in preventing the bacterial adhesion of *Escherichia coli* expressing YadaA, an adhesive protein from *Yersinia* so-called *Yersinia* adhesin. The use of design of experiments techniques allowed for successfully attaining a PET material with a high bacterial anti-adhesiveness, using a simple grafting approach.

Graphical abstract



Keywords: grafting, gum arabic, surface modification, wettability, hydrophilicity, design of experiments

1. Introduction

Bacterial adhesion in the medical context causes several problems including high expenditure and death. Among those, the risk of healthcare associated infections (HAI) is tremendously high. The European Centre for Disease Prevention and Control (ECDC) estimates that 8.9 million HAI occur each year in European Hospitals and long-term facilities combined. Additionally, around 30% of bacteria responsible HAI were found to be resistant to antibiotics [1] and biofilms are known to play a great importance in HAI, mainly due to their tolerance and resistance to antimicrobial agents. Once a planktonic bacterium approaches a surface, it can attach irreversibly and grow/produce biofilms in which bacterial cells are colonized within. [2]. Thus, it is clear that the materials surface adhesiveness is a critical factor impacting bacterial adhesion. One preventive approach can be the modification of such surfaces to reduce the risk of bacterial adhesion and ultimately the growth of biofilms, antimicrobial resistant bacteria and bacteria associated infections. Polyethylene terephthalate (PET) is one of the most popular polymers used in the medical context, due to its biocompatibility, hardness, stiffness, and biological, chemical and mechanical stability. PET applications in the medical field include sutures, heart valves, surgical meshes, scaffolds, urinary and bloodstream catheters [3,4]. Nevertheless, PET surfaces are also prone to bacterial contamination and further modifications are necessary to limit and/or prevent such contaminations [4]. An important factor to consider when modifying a surface is its hydrophilicity. It has been found that hydrophilic materials are more resistant to bacterial adhesion compared to hydrophobic ones [5]. Polysaccharides comprise a polymeric group commonly used for surface modification mainly because of their hydrophilic characteristics. Some widely studied examples like hyaluronic acid [6], heparin [7], dextran [8], chitosan [9] have shown potential to decrease the bacterial adhesion and from those, heparin and hyaluronic acid modified materials are being commercially explored [7]. Another polysaccharide, gum Arabic, derived from *Acacia Senegal* and *Acacia Seyal* trees [10], is composed of less than 3% protein and more than 97% of polysaccharide [11], being the polysaccharide part constructed from neutral sugars (rhamnose, arabinose and galactose) and acids (glucuronic acid, 4-methoxyglucuronic acid) [10]. Gum Arabic has already been used to cover inflamed surfaces, burns, nodular leprosy, as well as treatment of bedsores and wounds traditionally [10]. Moreover, gum Arabic has been evaluated in hydrogel studies [12] and membrane biofouling studies where the membrane was prepared and casted with polymer blends [11]. The membrane blend studies showed that gum Arabic was an effective component at preventing bacterial adhesion due to its antimicrobial properties and hydrophilic nature [13]. Additionally, gum Arabic is negatively charged [14] which is another important factor that impacts bacterial adhesion. Since most bacteria are negatively charged, they adhere less on negatively charged surfaces due to formation of a negative double layer [15]. Therefore, gum Arabic, a natural polysaccharide, might also provide effective anti-adhesive/antifouling properties to PET, when subjected to a chemical modification process such as grafting.

Chemical reactions are affected by several parameters and statistical design of experiments (DoE) has proven to be a powerful tool to study individual factors and their interactions in a complex, multivariable system. The traditional experimental design, known as OFAT (one-factor-at-a-time), studies one factor/variable at a time, being an inefficient method due to the unnecessarily large number of experimental runs and the inability to study interactions among the factors [16]. Despite its well-known advantages, the use of DoE to evaluate and optimize surface hydrophilicity using contact angle as a

response variable is not common. Still, some studies have employed DoE approaches and contact angle as a response variable, when investigating several surface modification technologies, such as atmospheric plasma [17], microwave plasma [18] and surface initiated polymerization [19].

In this study, we aimed to modify PET surface with gum Arabic using glutaraldehyde as the crosslinker. A full factorial DoE was performed to access the impact of reaction time, reaction concentration, curing temperature and curing time, as well as the interaction of those parameters in the surface hydrophilicity of PET determined by the water contact angle (WCA) measurement. Using the optimal conditions defined by the models, modified PET surfaces were prepared to be further characterized regarding their ability to prevent bacterial adhesion, as well as other properties including roughness and topography. To the best of our knowledge, the work herein reported is the first study using gum Arabic for PET surface modification by grafting.

2. Materials and Methods

2.1 Materials

PET film (Mylar® A with thickness of 36 μ) was acquired from Isovolta Group. Glutaraldehyde (50% solution), spray dried gum Arabic (*Acacia* tree), ethylene diamine ($\geq 99\%$) and diodomethane (99%) were purchased from Sigma-Aldrich; hydrochloric acid (37%) from Fisher Chemicals; ethylene alcohol (99.5%) from Aga; sodium hydroxide from Eka, orange II dye from Acros Organics Luria Broth (LB) from NZYTech; agar powder from VWR chemicals; Isopropyl β -D-1-thiogalactopyranoside (IPTG) from Grisp; anhydrotetracycline hydrochloride from Fluka; kanamycin from Fisher Bioreagents and ampicillin from Applichem Panreac.

2.2 Pre-treatment

Thin PET films were cut into 6 X 9 cm rectangles and immersed in ethyl alcohol for 15 min and afterwards rinsed with ethyl alcohol, to clean the surface prior to functionalization. In order to create amine groups on the surface of PET, the films were aminolysed using a protocol reported elsewhere [20] and kept in 50% aqueous diamine solution at 40°C for 24 h which enabled the formation of amine groups at the PET ester linkage. Following the aminolysation process, the PET films were rinsed with distilled water and air dried prior to the crosslinking process. The functionalized samples were immersed in 4% glutaraldehyde aqueous solution with 0.5% 0.1M HCl (pH = 2.4). After 3.5 h at 40°C under continuous agitation at 100 rpm, the samples were removed from the solution, put into the oven and kept for 1 h at 120°C for curing. Afterwards, the samples were rinsed with distilled water, immersed in water for 3 h and rinsed again with plenty of distilled water.

2.3 Grafting of Gum Arabic

Pre-treated PET samples were placed in a distilled water solution with a pre-defined gum Arabic concentration, ranging from 1% to 5% for a given period of time, as defined in Table 1. The ranges for the different parameters were defined according to previous preliminary experiments (*data not shown*). Afterwards, gum Arabic samples were removed from solution and put in the oven to be cured at different temperatures and times, according to Table 1. Samples were then rinsed with plenty of distilled water and air dried at room temperature.

2.4 Experimental Design and Optimization by Response Surface Methodology (RSM)

In a first step, a 2^4 full factorial design was performed to evaluate the effect of several reaction parameters on PET grafting and later the design was augmented using a central composite design. For statistical calculation, the variables were coded according to Eq. (1):

$$x_i = (X_i - X_0) / \Delta X_i \quad (\text{Eq. 1})$$

where x_i is the independent variable coded value, X_i is the independent variable real value, X_0 is the independent variable real value on the center point and ΔX_i is the step change value. The selected variables and their levels are listed in Table 1. Due to constraints in the independent variables curing time (B) and reaction time (D), the minimum level tested in the central composite design had to be adjusted.

Minimum curing time and reaction time were set at 5 min (0.08 h), so the coded value changed from $-\sqrt{2}$ (-1.414) to -1.280 for curing time and from $-\sqrt{2}$ (-1.414) to -1.131 for the reaction time.

State-Ease® 'Design Expert' (version 12) software was used for regression and graphical analyses of the data obtained. The statistical significance of the regression coefficients was determined by Student's *t*-test, the second-order model equation was determined by Fischer's test and the proportion of variance explained by the model obtained was given by the multiple coefficient of determination, R^2 . The optimum range of the variables were obtained by the graphical and numerical analysis using the 'Design expert' program, based on the criterion of desirability.

(TAB 1)

2.5 Water Contact Angle (WCA)

The hydrophilicity of the modified surfaces was evaluated by static WCA measurement using the Optical Tensiometer Attension Model Theta Basic by Biolin Scientific, at room temperature. MiliQ water with a droplet size of 3 μ L was used. The measurements were repeated at least 4 times for each sample at different locations. Contact angle measurements were also performed with diiodomethane. Owens-Wendt-Rabel&Kaelble Model (OWRK) equation was used to calculate polar and disperse components of surface energy by using contact angle values from water and diiodomethane.

2.6 Acid Orange Colorimetric Method

Acid orange coloration was used for the determination of the presence of amino groups on the substrate's surface. The method used was adapted from Gallego et al. [21]. Samples with 2.5 X 2.5 cm were immersed in 6 mL of dye solution in acidic conditions (0.028g/L, pH=3 adjusted with HCl 37% in MiliQ water) and agitated at 100 rpm, at 40° C. Following that, samples were removed and rinsed intensively with aqueous acidic solution (pH = 3) to remove unbound dye. The absorbed dye was subsequently desorbed by immersing the films in an alkaline NaOH solution, at pH = 12 and then the absorbance of the final solution was measured in a Perkin Elmer Lambda 35 UV-VIS Spectrophotometer using an incident wavelength of 484nm.

2.7 ATR-FTIR

Fourier Transform Infrared Spectrophotometer (FTIR), Perkin Elmer Spectrum 100, with universal attenuated total reflectance (ATR) accessory with diamond crystal was used. The spectra were collected between the region of 4000 – 600 cm^{-1} wavenumbers with a 4 cm^{-1} resolution.

2.8 SEM

The morphological analyses of the samples were performed using a Scanning Electron Microscope NanoSEM - FEI Nova 200 (FEG/SEM) with a secondary electron detector with 10 KeV energy and a working distance between 7 and 8 mm. Before the morphological analysis, the samples were coated with a thin film of Au/Pd (80/20 by weight) 10 nm thick. For each sample, several images were taken by SEM, referring to different magnifications.

2.9 AFM

A Keysight Technologies 5500 Atomic Force Microscope was used to perform the AFM measurements. The measurements were performed in air in tapping mode (Mac Mode) at room temperature. The silicone material cantilevers with a spring constant of 13-77 N/m and radius < 10 nm were used. The images were analysed by the Keysight PicoView and Gwyddion software. All images were taken at 5µm X 5µm surface area.

2.10 Bacterial Adhesion

2.10.1 Bacterial Strains

E. coli BL21 (DE3) expressing green fluorescent protein (GFP) and an adhesive protein from *Yersinia* so-called *Yersinia* adhesin A (YadA), was used to test bacterial adhesion in the materials. The plasmid pRSFduet_GFP was kindly provided by Maria Sande (unpublished) and was obtained by amplification of GFP from pETduet_GFP (mut3b) [22]. The plasmid pASK_IBA2_YadA was kindly provided by Dirk Linke [23].

2.10.2 Preparation of Bacteria

E. coli BL21 DE3 (NZYTech, #MB006) harboring pRSFduet_GFP and pASK_IBA2_YadA, was cultivated at 37 °C, 200 rpm in LB medium (10 g/L tryptone, 5 g/L yeast extract, 10 g/L NaCl) with the addition of kanamycin (50 µg/mL) and ampicillin (100 µg/mL). For the adhesion experiments, the cultures were grown at 37°C and 200 rpm in LB (150 mL) up to an optical density at 600 nm (OD_{600nm}) of 0.6. Isopropyl β-D-thiogalactopyranoside (IPTG) and anhydrotetracycline (aTc) were added (final concentration of 1 mM and 100 ng/mL, respectively) to induce the heterologous protein expression (GFP and YadA). The cultures were then incubated for 5 h at 37 °C and 200 rpm. Next, the cells were harvested by centrifugation at 5000 rpm for 5 min and washed two times with 1 X PBS (phosphate buffer saline). Afterwards, the bacterial concentration was adjusted to an OD_{600nm} of 0.8 using 1 X PBS.

2.10.3 Bacterial Adhesion Test

Prior to the test, modified and unmodified PET film samples were cut into 1 X 1.5 cm size rectangles. To ensure reproducibility of the results, three replicates of each sample were prepared. The samples were immersed into 1% detergent solution and placed in an ultrasonic bath for 1 min, rinsed with water to remove contaminants and any possible previously attached microorganism. After that, samples were air dried in the flow chamber and UV treated for 30 min. Each sample was then placed into a falcon tube containing 14 mL of bacterial cells already prepared (OD_{600nm} of 0.8) and were incubated at 4°C for 4 h in an orbital shaker at 12 rpm. After incubation, PET samples were removed and washed gently with 1 X PBS buffer to remove unattached bacteria. The bacteria adhered on PET surfaces were visualized using a fluorescence microscope (Olympus BX51), at 60X magnification, coupled with an DP71 digital camera. Fluorescence imaging was done with 470-490 nm excitation and a 520 nm filter in the microscope optical path.

3. Results and Discussion

3.1 Water Contact Angle (WCA) Analysis of PET Control

WCA gives an indication about the wettability of the surface. However, some environmental conditions like dirt [24], humidity [25] and temperature [26,27] can affect the WCA. Thus, it is normal to expect some variations among each measurement. ~~To understand the variability observed in the WCA determination, the Shewhart control charts were obtained for untreated PET (PET control) sample, where~~

individual measurements were registered. The Shewhart Chart is illustrated in Figure 1, showing an average WCA of $70^\circ \pm 5$ was found for PET control of $70^\circ \pm 5^\circ$, in close agreement with other values found in literature for pristine PET (e.g. 72° [28] or 77° [21]). The values follow a normal distribution, showing that all the individual measurements fall within the control limits.

(FIG 1)

A surface with a high hydrophilicity behavior (i.e. low contact angle) exhibits a great potential as an anti-adhesive surface thus highlighting the need to further functionalize PET films and one of the commonly used approach is the grafting method to immobilize natural substances including polysaccharides [29].

3.2 Pre-treatment of PET substrate

Aminolysis of PET involves a reaction of primary amines with the ester linkage of PET which results in the formation of an amide linkage and hydroxyl group by chain cleavage [20,30]. By using diamine, free primary amine ending groups on the surface of PET were obtained, that can be available for further reaction for gum Arabic attachment (Figure 12).

(FIG 12)

The aminolysed PET samples were evaluated by ATR-FTIR and the acid orange coloration method in order to characterize the presence of amine groups on the surface. The ATR-FTIR data in Figure 23 shows stretching of the amide groups at 1649 cm^{-1} (amide I, C=O stretching) and 1548 cm^{-1} (amide II, NH deformation) on PET sample [31,32]. Although there were no medium or strong bands representative of the stretching of amine groups between $3000\text{--}3600\text{ cm}^{-1}$, the broad weak peak observed between $3000\text{--}3600\text{ cm}^{-1}$ can be due to presence of exchangeable protons from hydroxyls and amines. However, with a penetration depth as low as $0.6\text{ }\mu\text{m}$ [31], ATR-FTIR lacks high sensitivity for the thin surface modifications. Therefore, it can be assumed that the existence of characteristic peaks in the ATR-FTIR spectrum indicates some degree of bulk material modification, which is also supported by the literature [21,33].

(FIG 23)

Additionally, the presence of free amines was also confirmed with a colorimetric method. Acid orange has affinity to primary amine groups in acidic conditions due to electrostatic interactions occurring between the dye and amine groups [34]. The dye treated PET samples can be seen in Figure 34. The aminolysed samples showed a higher amount of dye absorption, meaning that the aminolysed samples obtained orange color after the dye application, indicating the presence of primary amine groups, as found also in previous studies [21,34].

(FIG 34)

Further modification of the aminolysed surfaces was performed with glutaraldehyde. Glutaraldehyde is a well-known crosslinker. The possible crosslinking of glutaraldehyde with amine groups and gum Arabic is shown in Figure 12. It is expected that glutaraldehyde forms Schiff bases with the amine groups. Although Schiff bases can be considered unstable and the exact mechanism is still unknown [35], several reports have shown that the bonds created by glutaraldehyde can be stable due to bulky hydrophobic part near to amine part of Schiff bases [36], or further reaction of the Schiff bases with glutaraldehyde [37]. It is also possible that the monomeric cyclic hemiacetal and multimeric cyclic hemiacetal form of glutaraldehyde react with the amine groups on the surface since this form is more likely to be stable in acidic conditions [35]. In order to evaluate glutaraldehyde modification, glutaraldehyde treated samples were further characterized with acid orange colorimetric assay, whereas the low absorbance of the orange

dye indicates the reduced amount of primary amine groups on glutaraldehyde treated samples as shown in Figure 34, thus confirming the bonding of glutaraldehyde on aminolysed PET surfaces. It was also observed that there was a slight yellow interference on the glutaraldehyde treated samples which may be due to the formation of Schiff bases [38–40]. Moreover, further characterization of the surfaces using water contact angle led to values of $64 \pm 1^\circ$ and $75 \pm 6^\circ$ for aminolysed and glutaraldehyde modified samples, respectively.

3.3 Statistical Analysis of Reaction Parameters

Organic reactions can be highly affected by the reaction parameters such as reaction time, reagents concentration and curing conditions. In a first step, screening experiments were conducted to identify the factors that influence PET grafting efficiency and to verify if any changes to their settings should be made to improve the process. The effects of different experimental variables on PET grafting process were simultaneously investigated, using a full factorial design experiment (Table 2, block 1). Four variables (curing temperature, curing time, gum Arabic concentration and contact time) were taken into account. The pre-treatment methods (glutaraldehyde modification and aminolysis) were performed for all the samples in the same conditions. The grafting process was then performed in aqueous solutions with 0.5% 0.1M HCl (pH values ranged between 3.4 and 4) at 40°C , where the grafting parameters were varied according to the design planning.

The initial WCA and WCA after 5 and 10 washing cycles (one cycle of washing consisted of immersing the sample in distilled water at 40°C , 100 rpm agitation for 30 mins) were chosen as the response variables. At least four measurements were performed in different locations of the sample, being the average values and standard deviation presented as the final response. The experimental matrix and the results for the factorial design are shown at Table 2 (block 1).

(TAB 2)

After the grafting reaction in the conditions set by the planning, the obtained PET grafted films were washed for 5X or 10X successively, to understand the resistance and stability of the produced gum Arabic coatings. After each washing cycle, the samples were removed and placed in a new container for another washing cycle. After 5 or 10 consecutive cycles, the samples were allowed to air dry and WCA was measured in the dried samples.

As can be observed in Table 2, the initial WCA after the functionalization process varied considerably (from 21° to 58°), being this variation identical after washing (from 29° to 58° and to 59° , after 5 and 10 washing cycles, respectively). However, higher average WCA were observed after washing (the mean WCA increased from 41° to 45° and 48° , after 5 and 10 washing cycles, respectively). The increase in the WCA with washing was expected, due to the low stability of the coating in some assay conditions and due to the presence of unreacted components that are being removed during the washing process. However, comparing with PET control samples that have a mean WCA of 70° , a significant decrease in the WCA was achieved after grafting and washing, being concluded that a stable grafting was achieved. Table 2 also shows that, independently of the other variables, increasing curing temperature from 80°C to 120°C resulted in a decrease of the WCA, and consequently, in a higher efficiency in the gum Arabic linkage. Finally, it is also possible to observe that lower WCA occurred when higher curing temperatures and times (more intense curing conditions) were used. Indeed, curing temperature (A) and curing time (B) have played a critical role in PET coating.

According to the Student's *t-test* results, the most important factors affecting the initial WCA were the curing temperature (A) and curing time (B), as can be observed in the half-normal probability plot (Figure 5), thus these factors were considered for building the linear model. Factor C, concentration, the first

order interactions AB and AC and the fourth order interaction ABCD were also considered in the linear model, due to their *t-test* value (above *t-value* limit).

(FIG 5)

Using the selected factors for building the linear model, the *Fischer's test* was used to evaluate the model significance. The ANOVA statistical analysis for the initial WCA is summarized in Table 3. A model *F-value* of 28.15 implies the model is significant (*p-value* < 0.0001), i.e. there is only a 0.01% chance that an *F-value* this large could occur due to noise.

(TAB 3)

The curvature and residual lack of fit were found to be insignificant, and the proportion of variance explained by the model, given by the multiple coefficient of determination, R^2 was found to be 0.9337, highlighting the model adequacy to predict the WCA in the design space. The obtained final model equation for the initial WCA, in terms of coded factors is:

$$\text{Initial WCA} = 41.11 - 7.63A - 5.25B + 2.37C - 3.50AB - 3.12AC + 3.38ABCD \quad (\text{Eq. 2})$$

Figure 46 shows the 3D surface for the initial WCA, where a clear interaction effect between curing temperature and curing time is observed, thus suggesting lower WCAs values when these 2 factors are simultaneously maximized.

(FIG 46)

The same statistical analysis was performed for the WCA after 5 and 10 washing cycles, being the *Fischer's test* used for evaluating the model significance and the ANOVA statistical analysis summarized in Table 4.

(TAB 4)

Although the obtained models were found to be statistically significant with 99.76% and 99.51% of probability for WCA 5X and WCA 10X respectively, and lack of fit was insignificant, they both presented curvature and a low coefficient of determination, R^2 . Consequently, the linear model is not adequate to navigate in the design space and an augmented design is recommended.

A Central Composite Design (CCD), with α equal to $\pm\sqrt{2}$ (± 1.414) was chosen to expand the model surface, with the time constraints already described. Table 2 block 2 shows the responses obtained for the WCA. When expanding the model, a similar variation of the WCA was found, where initial WCA varied from 21 to 58, and WCA 5X and 10 X varied from 29 to 61 and to 59, respectively.

The same statistical analysis was performed for the initial WCA and WCA after 5 and 10 washing cycles, being the *Fischer's test* used to evaluate the model significance. The *p-value* of obtained models were found to be statistically significant with *p-value* < 0.0001, *p-value* = 0.0002 and *p-value* = 0.0004 for WCA, WCA 5X and WCA 10X respectively. Their ANOVA statistical analysis are summarized in Table 5. Finally, Figure 57 shows the contour surfaces obtained for these responses, where it is clearly visible the need to increase curing temperature and curing times, to achieve low values for the WCA.

(TAB 5)

(FIG 57)

The curvature and residual lack of fit were found to be insignificant to all the responses analyzed and the residuals analysis were found to be normally distributed, thus indicating that the statistical studies could be continued with optimization. The predicted model equations for the initial WCA, WCA after 5 washing cycles and WCA after 10 washing cycles, in terms of coded factors, are:

$$\text{Initial WCA} = 39.79 - 7.94A - 5.54B - 6.71C - 3.50AB - 3.12AC + 9.09A^2C + 3.38ABCD \quad (\text{Eq. 3})$$

$$\text{WCA 5X} = 45.48 - 5.05A - 4.93B - 2.75BC + 3.37ACD + 2.88ABCD \quad (\text{Eq. 4})$$

$$\text{WCA 10X} = 47.22 - 8.83A - 3.21B + 2.44C + 2.62AC + 2.63ABD + 3.37ACD + 5.46AB^2 + 3.87ABCD \quad (\text{Eq. 5})$$

3.4 Optimization and characterization of the optimized PET surfaces

To improve the gum Arabic grafting process, the graphical optimization tool from Design-Expert® was used, being the objective, the minimization of the responses found for the WCA. The upper limits (corresponding to the minimum WCA) were set as 35° for WCA 0X and 42° for both WCA 5X and WCA 10X, since it is generally recognized that the improved washing resistance of the coatings is an indication of the efficiency of the grafting process. Ideally, after the first 5 consecutive washing cycles, the WCA should stay constant, meaning that the coating is stable, and no more chemicals are being released from the grafted surface.

Figure 68A shows the overlay plot of factor Curing time (B) versus Temperature (A) for the responses fulfilling simultaneously these criteria (yellow area). Observing the yellow shaded area, it is possible to conclude that using combined curing temperatures above 110°C and curing times higher than 2 h would enable achieving the desired WCA. As such, the study was continued setting the curing conditions at the following parameters: curing temperature of 120°C and curing time of 3 h. To aid the decision on the best gum Arabic concentration, the Overlay plot of factor C versus factor A (Figure 68, B) was analyzed, keeping factor B (curing time) at 3 h.

(FIG 68)

Analyzing Figure 68B, we can conclude that the range of gum Arabic concentrations for gum Arabic to fulfill the set criteria can go from 1% to approximately 4%. Since the minimization of consumables is always desired to decrease costs, the validation experiment was performed using 1% of gum Arabic and with 1 h of contact time for the grafting process, whereas the obtained coating would be cured at 120°C for 3 h. Under these conditions, a final validation trial was performed, and the obtained and predicted responses are presented in Table 6.

(TAB 6)

These trials have confirmed the models obtained, since the achieved WCA are included in the 95% confidence prediction interval given by the design. A low WCA ($27^\circ \pm 8$) was obtained for their optimized treated samples, and after washing, the developed coatings still presented low values for the WCA ($32^\circ \pm 8$ for 5X and $30^\circ \pm 7$ for 10X), which is correlated with the enhanced grafting performed. Further characterization experiments were conducted on the optimized samples, to assess their efficiency as anti-adhesive materials. Table 57 shows the surface energy for PET control and PET treated samples.

(TAB 57)

Besides ~~Additionally~~, to contact angle characterization, surface energy was calculated since several studies pointed out that the surface energy values of materials can be related with bacterial adhesion [41,42]. According to Owens-Wendt-Rabel&Kaelble Model (OWRK) equation, the polar and disperse surface energy values of treated and untreated samples can be calculated by using water and diiodomethane contact angles. Analyzing ~~according to~~ data shown in Table 57, it can be seen that polymers have a relatively high disperse component and low polar component of total surface energy. This is thought to be a characteristic behavior of the polymers [43]. However, after the surface treatment, an increase in the total surface energy from 49 mJ/m² to 70 mJ/m² and an increase in the polar component of surface energy from 7 mJ/m² to 29 mJ/m² has been observed. It is known that the water contact angle and surface energy are important parameters for bacterial adhesion tests, and the negative bacterial adhesion has been correlated with the polar component of surface energy and total surface energy for both gram negative and gram positive bacteria [41,44], where a material with a high total surface energy and with a high polar component correspond to the requirements towards a decreased bacterial adhesion. This kind of reduced adhesion can be explained with a strongly hydrated surface providing a physical and free energy barrier [45].

Gram negative bacteria like *E. coli* has a thinner peptidoglycan layer compared to gram positive bacteria and it provides less rigid surface which can promote adhesion on rough surfaces [29,46]. Topographical changes on PET surface is expected due to breakage (aminolysis) and formation of new bonds (attachment of glutaraldehyde and gum Arabic) via chemical reactions. Thus, the gum Arabic treated samples and untreated PET samples were further analyzed by SEM and AFM ~~analysis was further performed on the gum Arabic treated and untreated PET samples to verify if morphological changes occurred~~ in order to evaluate the effect of surface topography and verify the modification ~~The treated and untreated materials were analyzed under AFM in order to evaluate its surface topography~~ (Figure 79 and Figure 8). SEM images obtained from the surface included surface visualization with lower magnification and small morphological differences were observed (Figure 7) and AFM was utilized for further characterization ~~and closer look at the PET surface~~. As it can be seen from Figure 8, PET Control surface is smoother (with Ra = 7.24nm) when compared with the treated sample (Ra = 21 nm). In addition to Ra value, other parameters like kurtosis and skewness were further analyzed. While kurtosis can provide information about the sharpness of the peaks (if Rku>3, the peaks are sharp), the skewness value (Rsk) can indicate where the distribution is concentrated. The gum Arabic treated samples have a negative skew (Rsk = -0.867) which indicates that the data collected from the surface were skewed to negative side meaning that they have valleys constructed on the surface and it was also observed Rku<3 for both cases, indicating that the peaks were round [474].

(FIG 7)

(FIG 89)

3.5 Bacterial Adhesion on PET surfaces

Bacterial adhesion experiments were performed to study the effectiveness of the optimized gum Arabic treated PET surfaces. It is known that bacterial adhesins are involved in bacterial attachment and they further promote biofilm formation [485]. YadA is a *Yersinia* adhesin which promotes adhesion and auto-agglutination, thus suggesting its role in the biofilm formation by *Yersinia enterocolitica* [23]. Although bacterial adhesion mechanism of YadA is unknown, adhesins are known to play a role in maturation of adhesion and irreversible adhesion [48]. Moreover, it is also known to provide resistance to bactericidal activity [496]. In order to assess the adherence mediated by a highly adhesive adhesin like YadA in a low biosafety level laboratory, we assessed the adhesion of *E. coli* BL21 cells harboring pASK_IBA2_YadA

and pRSFduet_GFP using fluorescence microscopy where the material was immersed in the culture medium for 4 hours' incubation time.

(FIG 940)

It can be seen from Figure 940 that PET control sample was fully covered with bacteria after just 4 h of contact, as bacteria can strongly adhere onto surfaces as a key initial step in the formation of biofilms, whereas gum Arabic treated samples showed an extremely low number of adhered bacteria (almost residual). Thus, we can conclude that gum Arabic modified surface clearly exhibits anti-adhesive/antibacterial properties similarly to other polysaccharides reported for the same purpose [7–9]. The anti-adhesive/antibacterial properties of gum Arabic can be due to combination of some properties like hydrophilic nature [12], negative charge [14] and antimicrobial activities. Although the exact mechanism of antimicrobial action is unknown, there are some studies suggesting that the presence of antimicrobial enzymes like oxidases, peroxidases and pectinases might be the reason for its antimicrobial activity. Some other studies highlight that the presence of the high amounts of salts may be the reason for the antimicrobial properties of gum Arabic [5047,5148], since glucuronic acid is found as calcium, magnesium and potassium salts in nature [5249]. Furthermore, it was also seen that roughness obtained through modification did not promote the adhesion indicating that surface hydrophilicity can be more important at bacterial adhesion.

4. Conclusion

PET surface was modified with gum Arabic through treatments with diamines and glutaraldehyde. The use of WCA as a response for gum Arabic grafting onto PET films was used to find the optimum design parameters within the design of experiment range towards PET bacterial anti-adhesiveness. The parameters chosen were concentration, reaction time, curing temperature and curing time. It was found that curing temperature and curing time were the most significant parameters affecting the WCAs and their simultaneously maximization leads to a decrease of the WCA values. Using optimized conditions (1% GA concentration, 1 h of reaction time, curing temperature of 120°C and curing time of 3 h) an initial WCA of 27° was found. It was further shown that the treated samples were stable and resistant to several cycles of washings. Furthermore, the total surface energy and polar component of surface energy were found to be higher for treated samples, having increased from 49 mJ/m² to 70 mJ/m² and from 7 mJ/m² to 29 mJ/m², respectively. This corresponds to the requirements for obtaining a low bacterial adhesion on the surface. Finally, the bacterial adhesion susceptibility of treated and untreated materials was evaluated against *E. coli* expressing YadA, an adhesive protein from *Yersinia* so-called *Yersinia* adhesin A. The adhesion tests clearly showed that the treated materials were highly effective and resistant (numbers of bacteria adhered are residual), which could be explained by the low contact angle and/or bacterial inhibition properties of the gum Arabic and therefore, constitute promising materials to be further used in medical contexts.

5. Acknowledgements

This work was supported by the ViBrANT project that received funding from the EU Horizon 2020 Research and Innovation Programme under the Marie Skłodowska-Curie, Grant agreement no 765042 and the Portuguese Foundation for Science and Technology (FCT) under the scope of the strategic funding of UIDB/04469/2020.

6. References

- [1] C. Suetens, K. Latour, T. Kärki, E. Ricchizzi, P. Kinross, M.L. Moro, B. Jans, S. Hopkins, S. Hansen, O. Lyytikäinen, J. Reilly, A. Deptula, W. Zingg, D. Plachouras, D.L. Monnet, the H.-A.I.P.S. Group, Prevalence of healthcare-associated infections, estimated incidence and composite antimicrobial resistance index in acute care hospitals and long-term care facilities: Results from two european point prevalence surveys, 2016 to 2017, *Eurosurveillance*. 23 (2018) 1–17. <https://doi.org/10.2807/1560-7917.ES.2018.23.46.1800516>.
- [2] S.L. Percival, L. Suleman, C. Vuotto, G. Donelli, Healthcare-Associated infections, medical devices and biofilms: Risk, tolerance and control, *J. Med. Microbiol.* 64 (2015) 323–334. <https://doi.org/10.1099/jmm.0.000032>.
- [3] S. Rajendran, S.C. Anand, Woven textiles for medical applications, in: *Woven Text. Princ. Technol. Appl.*, 2012: pp. 414–441. <https://doi.org/10.1533/9780857095589.3.414>.
- [4] A. Subramaniam, S. Sethuraman, Biomedical Applications of Nondegradable Polymers, in: *Nat. Synth. Biomed. Polym.*, Elsevier Inc., 2014: pp. 301–308. <https://doi.org/10.1016/B978-0-12-396983-5.00019-3>.
- [5] Y.H. An, R.J. Friedman, Concise Review of Mechanisms of Bacterial Adhesion, *J. Biomed. Mater. Res.* 43 (1998) 338–348. [https://doi.org/10.1002/\(sici\)1097-4636\(199823\)43:3<338::aid-jbm16>3.0.co;2-b](https://doi.org/10.1002/(sici)1097-4636(199823)43:3<338::aid-jbm16>3.0.co;2-b).
- [6] L. Pérez-Álvarez, L. Ruiz-Rubio, I. Azua, V. Benito, A. Bilbao, J.L. Vilas-Vilela, Development of multiactive antibacterial multilayers of hyaluronic acid and chitosan onto poly(ethylene terephthalate), *Eur. Polym. J.* 112 (2019) 31–37. <https://doi.org/10.1016/j.eurpolymj.2018.12.038>.
- [7] G.A. Junter, P. Thébault, L. Lebrun, Polysaccharide-based antibiofilm surfaces, *Acta Biomater.* 30 (2016) 13–25. <https://doi.org/10.1016/j.actbio.2015.11.010>.
- [8] G. Xu, P. Liu, D. Prantyo, K.G. Neoh, E.T. Kang, Dextran- and Chitosan-Based Antifouling, Antimicrobial Adhesion, and Self-Polishing Multilayer Coatings from pH-Responsive Linkages-Enabled Layer-by-Layer Assembly, *ACS Sustain. Chem. Eng.* 6 (2018) 3916–3926. <https://doi.org/10.1021/acssuschemeng.7b04286>.
- [9] A. Verlee, S. Mincke, C. V. Stevens, Recent developments in antibacterial and antifungal chitosan and its derivatives, *Carbohydr. Polym.* 164 (2017) 268–283. <https://doi.org/10.1016/j.carbpol.2017.02.001>.
- [10] S.M. Al Alawi, M.A. Hossain, A.A. Abusham, Antimicrobial and cytotoxic comparative study of different extracts of Omani and Sudanese Gum acacia, *Beni-Suef Univ. J. Basic Appl. Sci.* 7 (2018) 22–26. <https://doi.org/10.1016/j.bjbas.2017.10.007>.
- [11] W. Falath, A. Sabir, K.I. Jacob, Novel reverse osmosis membranes composed of modified PVA/Gum Arabic conjugates: Biofouling mitigation and chlorine resistance enhancement, *Carbohydr. Polym.* 155 (2017) 28–39. <https://doi.org/10.1016/j.carbpol.2016.08.058>.
- [12] B. Singh, S. Sharma, A. Dhiman, Acacia gum polysaccharide based hydrogel wound dressings: Synthesis, characterization, drug delivery and biomedical properties, *Carbohydr. Polym.* 165 (2017) 294–303. <https://doi.org/10.1016/j.carbpol.2017.02.039>.
- [13] S. Sabri, A. Najjar, Y. Manawi, N.O. Eltai, A. Al-Thani, M.A. Atieh, V. Kochkodan, Antibacterial properties of polysulfone membranes blended with Arabic gum, *Membranes (Basel)*. 9 (2019) 29.

<https://doi.org/10.3390/membranes9020029>.

- [14] S. Asim, M. Wasim, A. Sabir, M. Shafiq, H. Andlib, S. Khuram, A. Ahmad, T. Jamil, The effect of Nanocrystalline cellulose/Gum Arabic conjugates in crosslinked membrane for antibacterial, chlorine resistance and boron removal performance, *J. Hazard. Mater.* 343 (2018) 68–77. <https://doi.org/10.1016/j.jhazmat.2017.09.023>.
- [15] M. Kiremitci-Gumusderelioglu, A. Peşmen, Microbial adhesion to ionogenic PHEMA, PU PP implants, *Biomaterials.* 17 (1996) 443–449. [https://doi.org/10.1016/0142-9612\(96\)89662-1](https://doi.org/10.1016/0142-9612(96)89662-1).
- [16] S.A. Weissman, N.G. Anderson, Design of Experiments (DoE) and Process Optimization. A Review of Recent Publications, *Org. Process Res. Dev.* 19 (2015) 1605–1633. <https://doi.org/10.1021/op500169m>.
- [17] E. Vazirinasab, R. Jafari, G. Momen, Evaluation of atmospheric-pressure plasma parameters to achieve superhydrophobic and self-cleaning HTV silicone rubber surfaces via a single-step , eco-friendly approach, *Surf. Coat. Technol.* 375 (2019) 100–111. <https://doi.org/10.1016/j.surfcoat.2019.07.005>.
- [18] A. Grandoni, G. Mannini, A. Glisenti, A. Manariti, G. Galli, Use of statistical design of experiments for surface modification of Kapton films by CF₄ –O₂ microwave plasma treatment, *Appl. Surf. Sci.* 420 (2017) 579–585. <https://doi.org/10.1016/j.apsusc.2017.05.140>.
- [19] R. Kumar, J. Lahann, Predictive Model for the Design of Zwitterionic Polymer Brushes: A Statistical Design of Experiments Approach, *ACS Appl. Mater. Interfaces.* 8 (2016) 16595–16603. <https://doi.org/10.1021/acsami.6b04370>.
- [20] N.P. Desai, J.A. Hubbell, Biological responses to polyethylene oxide modified polyethylene terephthalate surfaces, *J. Biomed. Mater. Res.* 25 (1991) 829–843.
- [21] S. Del Hoyo-Gallego, L. Pérez-Álvarez, F. Gómez-Galván, E. Lizundia, I. Kuritka, V. Sedlarik, J.M. Laza, J.L. Vila-Vilela, Construction of antibacterial poly(ethylene terephthalate) films via layer by layer assembly of chitosan and hyaluronic acid, *Carbohydr. Polym.* 143 (2016) 35–43. <https://doi.org/10.1016/j.carbpol.2016.02.008>.
- [22] J.L. Rodrigues, M. Sousa, K.L.J. Prather, L.D. Kluskens, L.R. Rodrigues, Selection of *Escherichia coli* heat shock promoters toward their application as stress probes, *J. Biotechnol.* 188 (2014) 61–71. <https://doi.org/10.1016/j.jbiotec.2014.08.005>.
- [23] P. Wollmann, K. Zeth, A.N. Lupas, D. Linke, Purification of the YadA membrane anchor for secondary structure analysis and crystallization, *Int. J. Biol. Macromol.* 39 (2006) 3–9. <https://doi.org/10.1016/j.ijbiomac.2005.11.009>.
- [24] Y. Yuan, T.R. Lee, Contact Angle and Wetting Properties, in: *Surf. Sci. Tech.*, 2013: pp. 3–34. https://doi.org/10.1007/978-3-642-34243-1_1.
- [25] M.J. Mackel, S. Sanchez, J.A. Kornfield, Humidity-Dependent Wetting Properties of High Hysteresis Surfaces, *Langmuir.* 23 (2007) 3–7.
- [26] J.D. Bernardin, I. Mudawar, B.W. Christopher, E.I. Franses, Contact angle temperature dependence for water droplets on practical aluminum surfaces, *Int. J. Heat Mass Transf.* 40 (1997) 1017–1033.
- [27] K.A. Emelyanenko, A.M. Emelyanenko, L.B. Boinovich, Water and Ice Adhesion to Solid Surfaces : Common and Specific , the Impact of Temperature, *Coatings.* 10 (2020) 648.

- [28] L.A. Gallarato, L.E. Mulko, M.S. Dardanelli, C.A. Barbero, D.F. Acevedo, E.I. Yslas, Synergistic effect of polyaniline coverage and surface microstructure on the inhibition of *Pseudomonas aeruginosa* biofilm formation, *Colloids Surfaces B Biointerfaces*. 150 (2017) 1–7. <https://doi.org/10.1016/j.colsurfb.2016.11.014>.
- [29] T. Çaykara, M.G. Sande, N. Azoia, L.R. Rodrigues, C.J. Silva, Exploring the potential of polyethylene terephthalate in the design of antibacterial surfaces, *Med. Microbiol. Immunol.* 209 (2020) 363–372. <https://doi.org/10.1007/s00430-020-00660-8>.
- [30] S. G. E. Sweet, B. J. P. Bell, Selective Chemical Etching of Poly(ethylene Terephthalate) Using Primary Amines, *J. Polym. Sci. Polym. Phys. Ed.* 16 (1978) 1935–1946.
- [31] M. Avadanei, Variable Angle ATR – FTIR Study of the Surface Aminolysis of Poly (Ethylene Terephthalate) Films, *J. Macromol. Sci. , Part B Phys.* 51 (2012) 425–437. <https://doi.org/10.1080/00222348.2011.597326>.
- [32] L. Bech, T. Meylheuc, B. Lepoittevin, P. Roger, Chemical Surface Modification of Poly (ethylene terephthalate) Fibers by Aminolysis and Grafting of Carbohydrates, *J. Polym. Sci. Part A Polym. Chem.* 45 (2007) 2172–2183. <https://doi.org/10.1002/pola>.
- [33] S. Noel, B. Liberelle, A. Yogi, M.J. Moreno, M.N. Bureau, L. Robitaille, G. De Crescenzo, A non-damaging chemical amination protocol for poly(ethylene terephthalate) – application to the design of functionalized compliant vascular grafts, *J. Mater. Chem. B.* 1 (2013) 230–238. <https://doi.org/10.1039/c2tb00082b>.
- [34] S. Noel, B. Liberelle, L. Robitaille, G. De Crescenzo, Quantification of Primary Amine Groups Available for Subsequent Biofunctionalization of Polymer Surfaces, *Bioconjug. Chem.* 22 (2011) 1690–1699.
- [35] I. Migneault, C. Dartiguenave, M.J. Bertrand, K.C. Waldron, Glutaraldehyde : behavior in aqueous solution , reaction with proteins , and application to enzyme crosslinking, *Biotechniques.* 37 (2004) 790–802.
- [36] M.A. Vazquez, F. Muroz, J. Donoso, Influence of the Side Chain on the Stability of Schiff-Bases Formed Between Pyridoxal 5 ' -Phosphate and Amino Acids, *Int. J. Chem. Kinet.* 22 (1990) 905–914.
- [37] L.H.H. Olde Damink, P.J. Dijkstra, M.J.A. Van Luyn, P.B. Van Wachem, P. Nieuwenhuis, J. Feijen, Glutaraldehyde as a crosslinking agent for collagen-based biomaterials, *J. Mater. Science Mater. Med.* 6 (1995) 460–472.
- [38] D. Hopwood, Some aspects of fixation with glutaraldehyde. A biochemical and histochemical comparison of the effects of formaldehyde and glutaraldehyde fixation on various enzymes and glycogen, with a note on penetration of glutaraldehyde into liver, *J. Anat.* 101 (1967) 83–92.
- [39] N. Nematidil, M. Sadeghi, S. Nezami, H. Sadeghi, Synthesis and characterization of Schiff-base based chitosan-g- glutaraldehyde / NaMMTNPs-APTES for removal Pb 2+ and Hg 2+ ions, *Carbohydr. Polym.* 222 (2019) 114971. <https://doi.org/10.1016/j.carbpol.2019.114971>.
- [40] M.I. Wahba, Chitosan-glutaraldehyde activated calcium pectinate beads as a covalent immobilization support, *Biocatal. Agric. Biotechnol.* 12 (2017) 266–274. <https://doi.org/10.1016/j.bcab.2017.10.016>.
- [41] M. Katsikogianni, E. Amanatides, D. Mataras, Y.F. Missirlis, Staphylococcus epidermidis adhesion to He, He/O₂ plasma treated PET films and aged materials: Contributions of surface free energy and shear rate, *Colloids Surfaces B Biointerfaces.* 65 (2008) 257–268.

<https://doi.org/10.1016/j.colsurfb.2008.04.017>.

- [42] Q. Zhao, S. Wang, H. Müller-Steinhagen, Tailored surface free energy of membrane diffusers to minimize microbial adhesion, *Appl. Surf. Sci.* 230 (2004) 371–378. <https://doi.org/10.1016/j.apsusc.2004.02.052>.
- [43] M. Kalin, M. Polajnar, The wetting of steel , DLC coatings , ceramics and polymers with oils and water : The importance and correlations of surface energy, surface tension, contact angle and spreading, *Appl. Surf. Sci.* 293 (2014) 97–108. <https://doi.org/10.1016/j.apsusc.2013.12.109>.
- [44] F. Rezaei, M. Abbasi-Firouzjah, B. Shokri, Investigation of antibacterial and wettability behaviours of plasma-modified PMMA films for application in ophthalmology, *J. Phys. D: Applied Phys* 47 (2014) 085401. <https://doi.org/10.1088/0022-3727/47/8/085401>.
- [45] A. M. C. Maan, A. H. Hofman, W. M. de Vos, M. Kamperman, Recent Developments and Practical Feasibility of Polymer-Based Antifouling Coatings, *Adv. Funct. Mater.*, 30 (2020) 2000936. <https://doi.org/10.1002/adfm.202000936>.
- [46] W. Pajerski, D. Ochonska, M. Brzychczy-Wloch, P. Indyka, M. Jarosz, M. Golda-Cepa, Z. Sojka, A. Kotarba, Attachment efficiency of gold nanoparticles by Gram-positive and Gram-negative bacterial strains governed by surface charges, *J. Nanoparticle Res.* 21 (2019) 186. <https://doi.org/10.1007/s11051-019-4617-z>
- [474] N. Duboust, H. Ghadbeigi, C. Pinna, S. Ayvar-Soberanis, An optical method for measuring surface roughness of machined Carbon Fibre Reinforced Plastic composites, *J. Compos. Mater.* 51 (2017) 289–302. <https://doi.org/10.1177/0021998316644849>.
- [485] C. Berne, A. Ducret, G.G. Hardy, Y. V. Brun, Adhesins Involved in Attachment to Abiotic Surfaces by Gram-Negative Bacteria, *Microb. Spectr.* 3 (2015). <https://doi.org/10.1128/microbiolspec.MB-0018-2015>.
- [496] Y. Schmid, G.A. Grassl, O.T. Bühler, M. Skurnik, I.B. Autenrieth, E. Bohn, *Yersinia enterocolitica* adhesin A induces production of interleukin-8 in epithelial cells, *Infect. Immun.* 72 (2004) 6780–6789. <https://doi.org/10.1128/IAI.72.12.6780-6789.2004>.
- [5047] M.A. Montenegro, M.L. Boiero, L. Valle, C.D. Borsarelli, Gum Arabic: More Than an Edible Emulsifier, in: *Prod. Appl. Biopolym.*, 2012. <https://doi.org/10.5772/33783>.
- [5148] A. Najjar, S. Sabri, R. Al-Gaashani, V. Kochkodan, M.A. Atieh, Enhanced fouling resistance and antibacterial properties of novel graphene oxide-arabic gum polyethersulfone membranes, *Appl. Sci.* 9 (2019). <https://doi.org/10.3390/app9030513>.
- [5249] E. Dauqan, A. Abdullah, Utilization of gum Arabic for industries and human health, *Am. J. Appl. Sci.* 10 (2013) 1270–1279. <https://doi.org/10.3844/ajassp.2013.1270.1279>.

Figure Captions

Figure 1. Shewhart chart for PET Control

Figure 12. Schematic representation of PET modification with gum Arabic

Figure 23. FTIR spectrum of unmodified PET (PET Control) and diamine treated PET (PET Amine)

Figure 34. Acid orange colorimetric assay; a) unmodified PET sample (PET Control), b) aminolysed PET sample (PET- Amine), c) glutaraldehyde modified aminolysed PET sample (PET-GTA), d) Absorption values from UV-vis spectroscopy for PET Control, PET-Amine and PET GTA

Figure 5. Half Normal Probability Plot for the factors and their interactions on the response Initial WCA

Figure 46. 3D graphical visualization of the initial WCA with factors A (curing temperature) and B (curing time). Factors C (gum Arabic concentration) and D (contact time) were kept at the central point

Figure 57. Contour Plots for factors A (curing temperature) and B (curing time), for the models attained for a) the initial WCA, b) WCA after 5 washing cycles and c) WCA after 10 washing cycles. Factors C (gum Arabic concentration) and D (contact time) were kept at the central point

Figure 68. Overlay Plots highlighting the area were responses fulfill the set criteria (initial WCA of 35° and WCA 5X and 10X of 42°). a) Factor B (Curing time) versus A (Temperature), keeping C=3% and D=8h (central point); b) Factor C (Gum Arabic concentration) versus A (Temperature), keeping B=3 h and D= 8h

Figure 7. SEM Images for samples a - c) PET Control, b – d) PET Gum Arabic treated samples at two different magnifications

Figure 89. AFM Images for the samples a - b) PET Control, c – d) PET Gum Arabic samples

Figure 910. Fluorescence microscopy images of *Escherichia coli* BL21 cells harboring pRSFduet_GFP and pASK_IBA2_YadA plasmids a) PET Control and b) PET Gum Arabic. Scale bar, 10µm

Table Captions

Table 1: Coded and actual levels for the variables studied in the central composite design

Table 2: Values for WCA after functionalization (OX), after 5 washing cycles (5X) and after 10 washing cycles (10X), according to the 2⁴ factorial design (block 1) and to the Central Composite Design (block 2), ordered by standard order

Table 3: Analysis of Variance (ANOVA) for the linear model obtained for the initial WCA

Table 4: Analysis of Variance (ANOVA) for the linear model obtained for WCA after 5 and 10 washing cycles

Table 5: Analysis of Variance (ANOVA) for the models obtained for the 3 responses analyzed: Initial WCA, WCA after 5 and WCA after 10 washing cycles

Table 6: WCA for Validated Samples (A=120, B=3, C=1, D=1)

Table 57: Surface Roughness and Energy of PET Control and PET Gum Arabic (Optimized Gum Arabic treated sample)

Journal Pre-proof

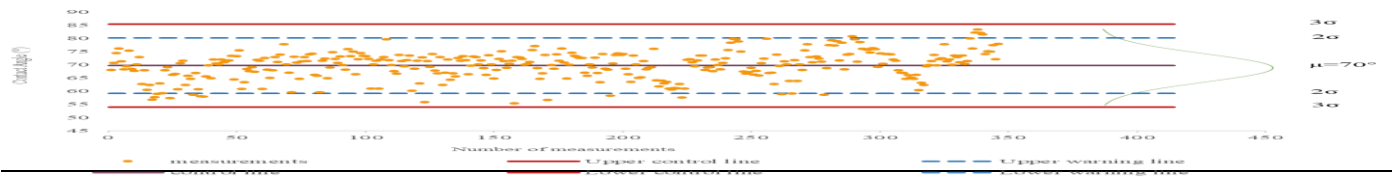


Fig.1.

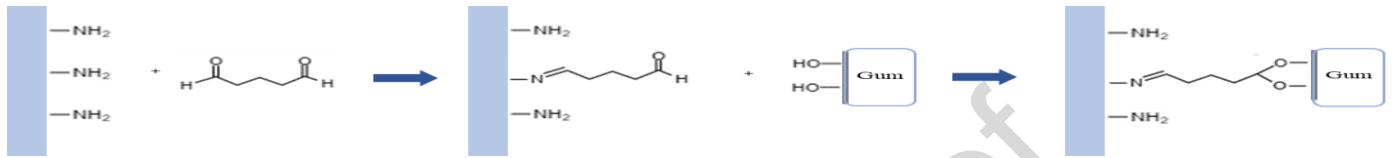


Fig.12.

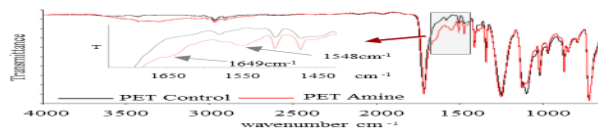


Fig.23.

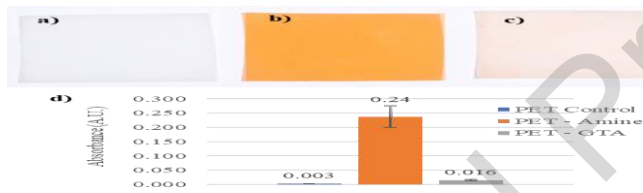


Fig. 34.

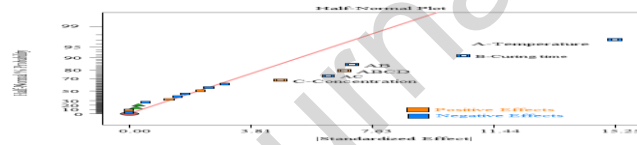


Fig. 5.

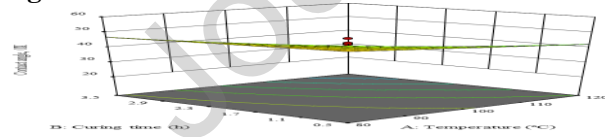


Fig. 46.

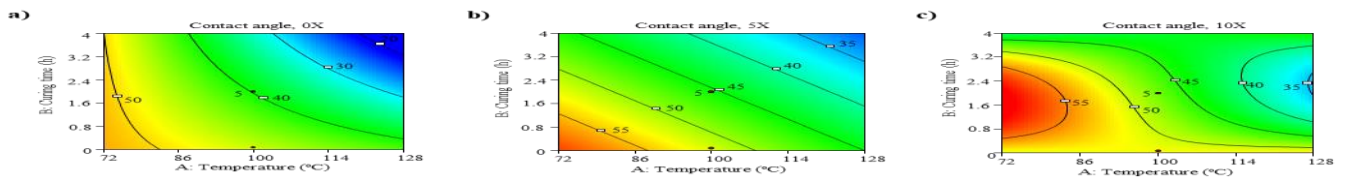


Fig. 57.

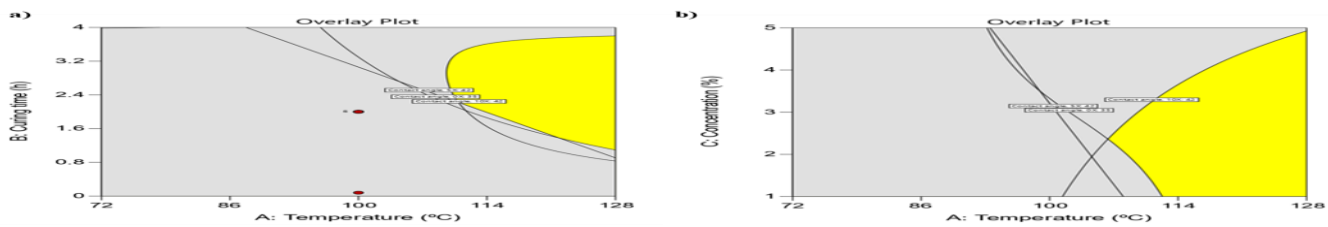


Fig. 68.

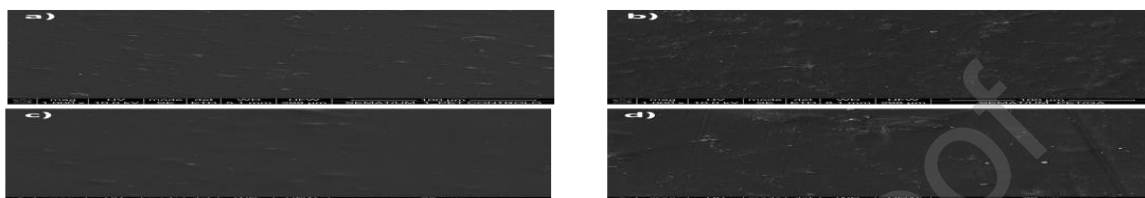


Fig. 7.

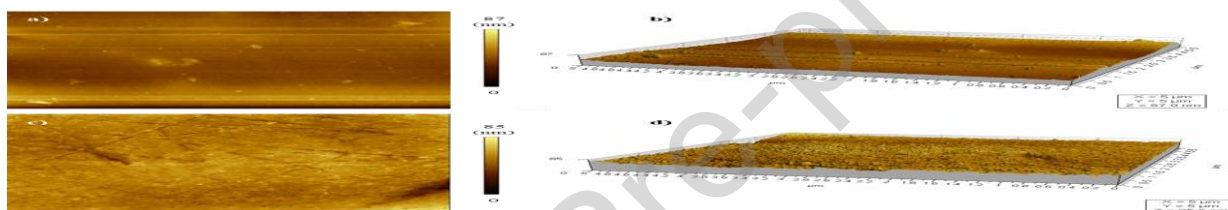


Fig. 89.

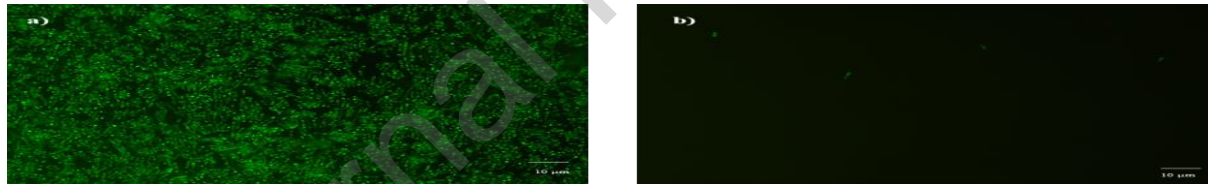


Fig. 910.

Table 1

Independent variables	Factor	Range and levels				
		-1.414	-1	0	+1	+1.414
Curing temperature (°C)	A	71.7	80	100	120	128.3
Curing time (hours)	B	0.08 (-1.280)	0.50	2	3.50	4.12
Reaction Concentration (%)	C	0.2	1	3	5	5.8
Reaction Time (hours)	D	0.08 (-1.131)	1	8	15	17.9

Table 2

Assay	Block	Variables				Responses		
		Curing temperature (°C)	Curing time (h)	Gum Arabic concentration (%)	Reaction time (h)	Contact angle (0X)	Contact angle (5X)	Contact angle (10X)
1	1	80	0.5	1	1	49±7	49±6	53±6
2	1	120	0.5	1	1	41±4	41±6	44±4
3	1	80	3.5	1	1	37±6	41±5	45±3
4	1	120	3.5	1	1	27±5	34±9	34±6
5	1	80	0.5	5	1	55±2	52±5	55±5
6	1	120	0.5	5	1	49±4	49±5	50±2
7	1	80	3.5	5	1	58±2	50±8	58±3
8	1	120	3.5	5	1	21±3	29±5	37±1
9	1	80	0.5	1	15	39±3	46±7	48±4
10	1	120	0.5	1	15	42±4	39±3	40±3
11	1	80	3.5	1	15	46±8	58±4	53±6
12	1	120	3.5	1	15	25±4	32±3	33±8
13	1	80	0.5	5	15	57±6	52±3	59±4
14	1	120	0.5	5	15	35±5	54±4	51±2
15	1	80	3.5	5	15	45±6	32±3	29±3
16	1	120	3.5	5	15	24±3	42±3	57±3
17	1	100	2	3	8	46±8	45±6	53±5
18	1	100	2	3	8	42±5	49±4	54±3
19	1	100	2	3	8	43±3	57±4	59±3
20	2	71.7	2	3	8	50±1	61±7	55±4
21	2	128.3	2	3	8	24±3	32±2	30±5
22	2	100	0.08	3	8	43±3	55±4	53±4
23	2	100	4.12	3	8	25±5	31±3	46±5
24	2	100	2	0.17	8	50±5	50±6	46±4
25	2	100	2	5.83	8	31±4	46±8	48±4
26	2	100	2	3	0.08	38±3	39±4	47±2
27	2	100	2	3	17.9	38±6	44±2	48±3
28	2	100	2	3	8	37±5	51±5	44±3
29	2	100	2	3	8	48±8	52±8	47±9

Table 3

Factors	WCA (0X)				
	Sum of Squares	df	Mean Square	F-value	p-value
Model	1996.0	6	332.67	28.15	< 0.0001
A	930.25	1	930.25	78.73	< 0.0001
B	441.00	1	441.00	37.32	< 0.0001
C	90.25	1	90.25	7.64	0.0172
AB	196.00	1	196.00	16.59	0.0015
AC	156.25	1	156.25	13.22	0.0034
ABCD	182.25	1	182.25	15.42	0.0020
Residual	141.79	12	11.82		

Lack of fit	133.12	10	13.31	3.07	0.2705
Pure error	8.67	2	4.33		
Cor Total	2137.79	18			

Table 4

Factors	WCA (5X)					Factors	WCA (10X)				
	Sum of Squares	Df	Mean Square	F-value	p-value		Sum of Squares	df	Mean Square	F-value	p-value
Model	997.50	6	166.25	7.31	0.0024	Model	1139.75	7	162.82	6.34	0.0049
A	225.00	1	225.00	9.89	0.0093	A	182.25	1	182.25	7.10	0.0237
B	256.00	1	256.00	11.26	0.0064	B	182.25	1	182.25	7.10	0.0237
AC	81.00	1	81.00	3.56	0.0858	C	132.25	1	132.25	5.15	0.0466
BC	121.00	1	121.00	5.32	0.0415	AC	110.25	1	110.25	4.30	0.0650
ACD	182.25	1	182.25	8.01	0.0163	ABD	110.25	1	110.25	4.30	0.0650
ABCD	132.25	1	132.25	5.82	0.0345	ACD	182.25	1	182.25	7.10	0.0237
Curvature	109.49	1	109.49	4.81	0.0506	ABCD	240.25	1	240.25	9.36	0.0121
						Curvature	191.58	1	191.58	7.46	0.0211
Residual	250.17	11	22.74			Residual	256.67	10	25.67		
Lack of fit	175.50	9	19.50	0.5223	0.7971	Lack of Fit	236.00	8	29.50	2.85	0.2852
Pure error	74.67	2	37.33			Pure Error	20.67	2	10.33		
Cor Total	1357.16	18				Cor Total	1588.00	18			

Table 5

Factors	Contact angle (0X)		Factors	Contact angle (5X)		Factors	Contact angle (10X)	
	Sum of squares	p-value		Sum of squares	p-value		Sum of squares	p-value
Block	47.95		Block	11.25		Block	16.77	
Model	2668.88	<0.0001	Model	1422.38	0.0002	Model	1459.18	0.0004
A	1260.43	<0.0001	A	510.29	0.0011	A	312.50	0.0033
B	603.2	<0.0001	B	476.59	0.0014	B	202.23	0.0142
C	180.50	0.0023	BC	121.00	0.0803	C	119.19	0.0521
AB	196.00	0.0016	ACD	182.25	0.0348	AC	110.25	0.0608
AC	156.25	0.0040	ABCD	132.25	0.0683	ABD	110.25	0.0608
A ² C	264.57	0.0004				ACD	182.25	0.0190
ABCD	182.25	0.0022				AB ²	95.44	0.0792
						ACBD	240.25	0.0084
Residual	295.31		Residual	791.68		Residual	527.22	
Lack of fit	226.14	0.8019	Lack of Fit	716.52	0.4159	Lack of Fit	502.06	0.1520
Pure error	69.17		Pure Error	75.17		Pure Error	25.17	
Cor Total	3012.14		Cor Total	2225.31		Cor Total	2003.17	

Table 6

Response	Predicted Mean	Std Dev	95% PI	Data Mean
Initial WCA	28.82	3.84	19.72 – 37.93	27 ± 8
WCA 5X	44.27	5.99	30.48 – 58.06	32 ± 8
WCA 10X	37.82	5.27	24.86 – 50.77	30 ± 7

Table 57

Samples	Surface Roughness			Contact Angle		Surface Energy		
	Ra (nm)	Skew	Kurtosis	Water Contact Angle (°)	Diodomethane Contact Angle (°)	SFE Polar (mJ/m ²)	SFE Disperse (mJ/m ²)	SFE Total (mJ/m ²)
PET Control	7.24	1.11	1.4	70° ± 5	34° ± 8	7 ± 3	42 ± 4	49 ± 4
PET Gum Arabic	21	-0.87	0.016	27° ± 8	38° ± 4	29 ± 2	41 ± 4	70 ± 4

Journal Pre-proof

Author statements:

Tugce Caykara – Conceptualisation, Methodology, Formal Analysis, Investigation, Writing - Original draft, Visualisation

José Silva - Investigation

Sara Fernandes – Writing & Review Editing

Adelaide Braga – Methodology, Investigation, Writing & Review Editing

Joana Rodrigues – Writing & Review Editing

Ligia R. Rodrigues – Resources, Writing & Review Editing, Supervision

Carla Silva – Formal Analysis, Resources, Writing & Review Editing, Visualisation, Supervision

Journal Pre-proof

Declaration of interests

The authors declare that they have no known competing financial interests or personal relationships that could have appeared to influence the work reported in this paper.

The authors declare the following financial interests/personal relationships which may be considered as potential competing interests:

Journal Pre-proof

- A statistical design of experiments approach was applied to optimize the modification of polyethylene terephthalate surface with gum Arabic by grafting
- The attained models for the response contact angle showed that this grafting procedure was affected the most by curing time and curing temperature.
- The surface hydrophilicity was enhanced with the optimized treatment by decreasing water contact angle from 70° to 27°.
- The treated surface has shown to be highly effective at reducing bacterial adhesion against *Escherichia coli* expressing YadA, an adhesive protein from *Yersinia* so-called *Yersinia* adhesin A.

Journal Pre-proof